

High-resistance liquid-crystal lens array for rotatable 2D/3D autostereoscopic display

Yu-Cheng Chang, Tai-Hsiang Jen, Chih-Hung Ting, and Yi-Pai Huang*

Department of Photonics & Institute of Electro-Optical Engineering, National Chiao Tung University, Hsinchu 30010, Taiwan

*boundshuang@mail.nctu.edu.tw

Abstract: A 2D/3D switchable and rotatable autostereoscopic display using a high-resistance liquid-crystal (Hi-R LC) lens array is investigated in this paper. Using high-resistance layers in an LC cell, a gradient electric-field distribution can be formed, which can provide a better lens-like shape of the refractive-index distribution. The advantages of the Hi-R LC lens array are its 2D/3D switchability, rotatability (in the horizontal and vertical directions), low driving voltage (~2 volts) and fast response (~0.6 second). In addition, the Hi-R LC lens array requires only a very simple fabrication process.

©2014 Optical Society of America

OCIS codes: (220.0220) Optical design and fabrication; (230.3720) Liquid-crystal devices.

References and links

1. B. Javidi and F. Okano, *Three-dimensional television, video, and display technologies*, (Springer-Verlag, 2002), pp. 461.
2. H. H. Refai, "Static volumetric three-dimensional display," *IEEE J. Displ. Technol.* **5**(10), 391–397 (2009).
3. M. Gately, Y. Zhai, M. Yeary, E. Petrich, and L. Sawalha, "A three-dimensional swept volume display based on led arrays," *IEEE J. Displ. Technol.* **7**(9), 503–514 (2011).
4. C. V. Berkel and J. A. Clarke, "Characterization and optimization of 3D-LCD module design," *Proc. SPIE*, vol. **3012**, pp. 179–187, 1997.
5. J. Y. Son and B. Javidi, "Three-dimensional image methods based on multi-view images," *IEEE J. Displ. Technol.* **1**(1), 125–140 (2005).
6. H. H. Refai, "Static volumetric three-dimensional display," *IEEE J. Displ. Technol.* **5**(10), 391–397 (2009).
7. M. Gately, Y. Zhai, M. Yeary, E. Petrich, and L. Sawalha, "A three-dimensional swept volume display based on LED arrays," *IEEE J. Displ. Technol.* **7**(9), 503–514 (2011).
8. J.-Y. Son and B. Javidi, "Three-dimensional image methods based on multi-view images," *IEEE J. Displ. Technol.* **1**(1), 125–140 (2005).
9. Y. Takaki, K. Tanaka, and J. Nakamura, "Super multi-view display with a lower resolution flat-panel display," *Opt. Express* **19**(5), 4129–4139 (2011).
10. Y. Takaki, "Multi-view 3-D display employing a flat-panel display with slanted pixel arrangement," *J. Soc. Inf. Disp.* **18**(7), 476–482 (2010).
11. W. Mphepo, Y.-P. Huang, and H.-P. D. Shieh, "Enhancing the brightness of parallax barrier based 3d flat panel mobile displays without compromising power consumption," *IEEE J. Displ. Technol.* **6**(2), 60–64 (2010).
12. C.-H. Chen, Y.-P. Huang, S.-C. Chuang, C.-L. Wu, H.-P. D. Shieh, W. Mphepo, C.-T. Hsieh, and S.-C. Hsu, "Liquid crystal panel for high efficiency barrier type autostereoscopic three-dimensional displays," *Appl. Opt.* **48**(18), 3446–3454 (2009).
13. M. Lambooji, K. Hinnen, and C. Varekamp, "Emulating autostereoscopic lenticular designs," *IEEE J. Displ. Technology* **8**(5 Issue 5), 283–290 (2012).
14. G. J. Woodgate, J. Harrold, A. M. S. Jacobs, R. R. Moseley, and D. Ezra, "Flat-panel autostereoscopic displays: characterization and enhancement," *Proc. SPIE* **3957**, 153–164 (2000).
15. R. Brott and J. Schultz, "Directional backlight lightguide considerations for full resolution autostereoscopic 3D displays," *SID Symposium Digest of Technical Papers*, **41**, Issue 1, pp. 218–221, 2010.
16. B. Lee and J. H. Park, "Overview of 3D/2D switchable liquid crystal display technologies," *Proc. SPIE* **7618**, 761806 (2010).
17. C. W. L. IJzerman, S. T. de Zwart, and T. Dekker, "Design of 2D/3D switchable displays," *SID Symposium Digest*, **36**, Issue 1, pp. 98–101, 2005.
18. Y. P. Huang, L. Y. Liao, and C. W. Chen, "2-D/3-D switchable autostereoscopic display with multi-electrically driven liquid-crystal (MeD-LC) lenses," *J. Soc. Inf. Disp.* **18**(9), 642–646 (2010).
19. S. Sato, "Liquid-crystal lens—cells with variable focal length," *Jpn. J. Appl. Phys.* **18**(9), 1679–1684 (1979).
20. H. W. Ren, Y. H. Fan, S. Gauza, and S. T. Wu, "Tunable-focus cylindrical liquid crystal lens," *Jpn. J. Appl. Phys.* **43**(2), 652–653 (2004).

21. H. W. Ren, D. W. Fox, B. Wu, and S. T. Wu, "Liquid crystal lens with large focal length tunability and low operating voltage," *Opt. Express* **15**(18), 11328–11335 (2007).
22. H. K. Hong, S. M. Jung, B. J. Lee, and H. H. Shin, "Electric-Field-driven LC lens for 3-D/2-D autostereoscopic display," *J. Soc. Inf. Disp.* **17**(5), 399–406 (2009).
23. Y. P. Huang and C. W. Chen, "Superzone fresnel liquid crystal lens for temporal scanning auto-stereoscopic display," *IEEE J. Displ. Technol.* **8**(11), 650–655 (2012).
24. C. W. Chen, Y. P. Huang, and P. C. Chen, "Dual direction overdriving method for fast switching liquid crystal lens on 2D/3D switchable auto-stereoscopic display," *IEEE J. Displ. Technol.* **8**(10), 559–561 (2012).
25. S. Sato, "Liquid-crystal lens-cells with variable focal length," *Jpn. J. Appl. Phys.* **18**(9), 1679–1684 (1979).
26. G. J. Woodgate and J. Harrold, "Key design issue for autostereoscopic 2-D/3-D displays," *J. Soc. Inf. Disp.* **14**(5), 421–426 (2006).
27. G. J. Woodgate and J. Harrold, "Efficiency analysis for multi-view spatially multiplexed autostereoscopic 2-D/3-D displays," *J. Soc. Inf. Disp.* **15**(11), 873–881 (2007).
28. O. H. Willemsen, S. T. De Zwart, M. G. H. Hiddink, and O. Willemsen, "2-D/3-D switchable displays," *J. Soc. Inf. Disp.* **14**(8), 715–722 (2006).
29. H. K. Hong, S. M. Jung, B. J. Lee, and H. H. Shin, "Electric-field-driven LC lens for 3D/2D autostereoscopic display," *J. Soc. Inf. Disp.* **17**(5), 399–406 (2009).
30. J. G. Lu, X. F. Sun, Y. Song, and H. P. D. Shieh, "2-D/3-D switchable display by Fresnel-type LC lens," *J. Displ. Technol.* **7**(4), 215–219 (2011).
31. Y. H. Fan, H. W. Ren, and S. T. Wu, "Switchable Fresnel lens using polymer-stabilized liquid crystals," *Opt. Express* **11**(23), 3080–3086 (2003).
32. Y. C. Chen, L. Y. Liao, Y. P. Huang, and H. P. Shieh, "Extremely-fast focusing gradient driven liquid crystal lens driven by ultra-low operating voltages," *International Display Manufacturing Conference 2011*, PS-028.
33. A. F. Naumov, G. D. Love, M. Yu. Loktev, and F. L. Vladimirov, "Control optimization of spherical modal liquid crystal lenses," *Opt. Express* **4**(9), 344–352 (1999).
34. H. Okumura, H. Fujiwara; H. Okumura and H. Fujiwara, "A new low-image-lag drive method for large-size LCTVs," *J. Soc. Inf. Disp.* **1**(3), 335–339 (1993).

1. Introduction

There is interest in pursuing more realistic images on displays permitted by advancements in technology. Because 3D displays provide depth information that is lacking in 2D displays, 3D displays play an important role in next-generation display technology. Autostereoscopic 3D displays have certainly entered the mainstream in recent years, thanks to the convenience of achieving the 3D effect without wearing glasses [1–10]. The most common methods in autostereoscopic 3D technology are fixed parallax barriers and lenticular lenses [11–14]. However, the 2D image quality is degraded by the use of these approaches; when the ability to switch between 2D and 3D display modes is a necessary function, the image quality in 2D mode must be maintained. In addition, the use of portable devices has been rising sharply for the past decade, and the displays of such devices do not only show images in the vertical direction but also offer the horizontal mode (Fig. 1). Therefore, rotatable functionality is a standard requirement for a portable 3D display.

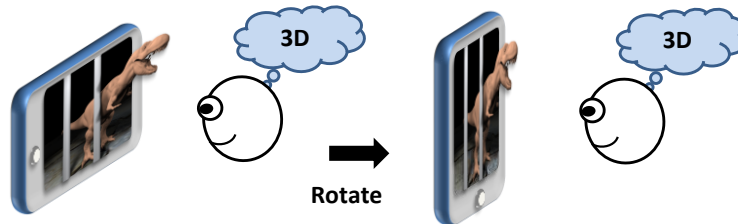


Fig. 1. A sketch of rotatable functionality.

There are several technologies can achieve 2D/3D switchable functionality, such as sequential backlight systems [15], switchable barriers [16] and switchable LC lenses [17–31]. Sketches and the various features of these technologies are shown in Table 1. The main advantage of sequential backlight technology is that it can provide a full-resolution 3D image to the observer. However, the viewing freedom in 3D mode is narrow; a 3D image can be shown only in the normal direction. In contrast, switchable barriers and switchable LC lenses can provide wider viewing freedom than sequential backlight systems. However, only switchable barriers and switchable LC lenses have the potential for rotatable functionality.

Nonetheless, the switchable barrier has a significant drawback: low brightness. Therefore, according to the above consideration of desirable features, an LC lens is the best candidate for mobile applications.

Table 1. Review of 2D/3D Switchable Technology

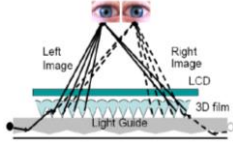
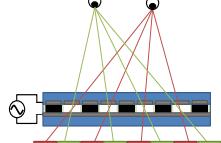
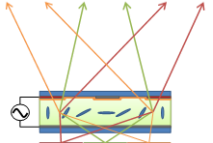
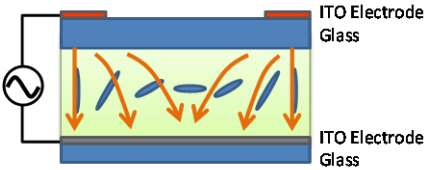
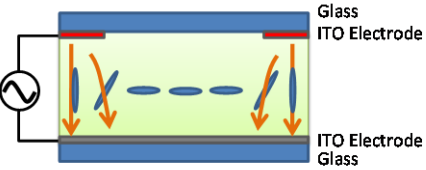
2D/3D Sequential Backlight	2D/3D Switchable Barrier	2D/3D Switchable LC Lens
 <ul style="list-style-type: none"> ✓ Full resolution ✗ Narrow viewing freedom 	 <ul style="list-style-type: none"> ✓ Simple process ✓ Wide viewing freedom ✗ Low brightness 	 <ul style="list-style-type: none"> ✓ Wide viewing freedom
 <p style="text-align: center;">(a)</p>	 <p style="text-align: center;">(b)</p>	

Fig. 2. Two electric-field-driven LC lenses (ELC lenses): (a) a structure with external electrodes and (b) a structure with internal electrodes.

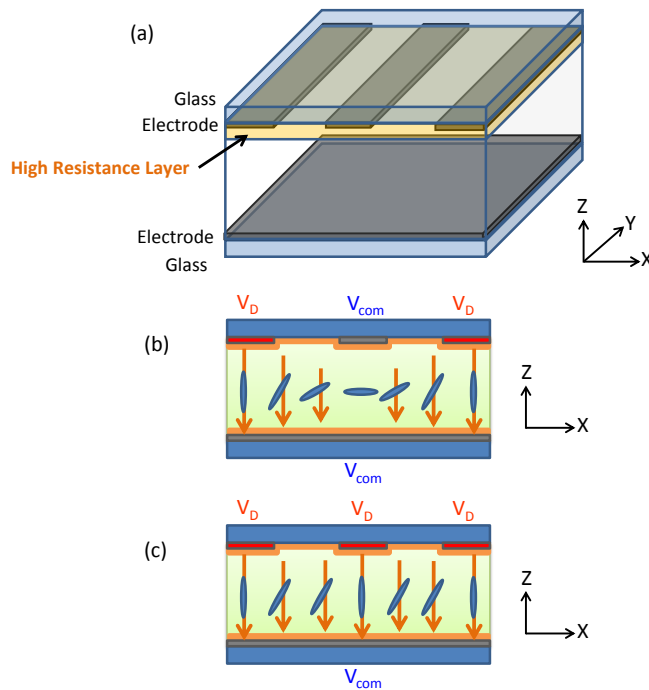


Fig. 3. Sketches of the high-resistance liquid-crystal lens (Hi-R LC lens): (a) the structure in perspective view, (b) the driving method for the lenticular lens, and (c) the driving method for the flat electrode.

Among current types of LC lenses, only an electric-field-driven LC lens (ELC lens) has the potential to yield 2D/3D rotation because it has no fixed physical lens structure. In a previous work, an external-electrode LC lens (Fig. 2 (a)) has been proposed that utilizes a glass substrate as a high-K material to smooth the electric field, producing a gradient distribution of the electric field in the LC cell. However, such a high-K material also increases the operating voltage (> 50 volts). Thus, an internal-electrode LC lens (Fig. 2 (b)), which can provide a lower operating voltage than the external-electrode lens, has been proposed [18]. However, without high-K material, the fringing electric field spreads only around the electrodes; therefore, the LC molecules in the central region are not driven, and an internal-electrode LC lens cannot form an ideal lens shape.

In this paper, we propose an internal-electrode LC lens with 2D/3D switchable and rotatable functionality by incorporating a high-resistance (Hi-R) layer [32]. The Hi-R LC lens is coated with a high-resistance layer within the cell, thus permitting the establishment of a continuous electric field with a gradient profile. In this manner, a lens-like profile can be formed. The most important concern when using a Hi-R layer is to avoid the electric-field distortions caused by crossed electrodes, thus maintaining high-performance 3D images in both the horizontal and vertical directions. A low operating voltage and fast switching time can be obtained using this design, as well. Moreover, the proposed Hi-R LC lens array requires only a very simple layout circuit with a similarly simple fabrication process.

2. High-resistance liquid crystal lens

2.1 Structure of single-layer Hi-R lenticular LC lens

Placing internal electrodes in an LC lens can yield lower driving voltages because the applied voltage can affect the LC molecules directly. However, because of the large slit between the electrodes, an internal-electrode LC lens can only share a weak electric energy and distribution of phase retardation. Most of the energy concentrates on the electrodes; the LC molecules can only be driven near the electrodes. Therefore, to overcome these issues, a high resistance-layer is coated onto the electrodes to generate a gradient voltage distribution in the LC cell. The LC molecules under the slits can also be affected by the electric field. As shown in Fig. 3(b), V_D and V_{com} are applied to the side and central electrodes of the LC lens, respectively. According to the function of the resistance layer, the voltage takes on gradient distribution on the resistance layer, and the voltage gradually changes from high to low for better phase retardation [33]. Therefore, the LC lens profile is not controlled by the fringing field but directly by the gradient voltage. In addition, if all electrodes on the same substrate are driven by V_{com} , the entire layer will perform as a flat ground electrode. As shown in Fig. 3(b) and Fig. 3(c), by changing the driving method, we can switch the electrodes from a strip to a flat form in the same layer.

2.2 Modeling of Hi-R LC lens

To further investigate the high-resistance LC lens, we construct an R-C circuit model to determine the parameters of the LC cell, as shown in Fig. 4. The resistance R in Fig. 4 is calculated using Eq. (1). To calculate the capacitance C in Fig. 4, the structure is first considered to be controlled by a uniform electrode field. The induced dipole moments of the two directions parallel and perpendicular to the LC direction are used. The equivalent polarization is shown in Eq. (2) and Eq. (3). The electric field is along the z direction, which induces the polarizations \vec{P}_{\parallel} and \vec{P}_{\perp} . The equivalent capacitance, C , can be calculated from χ_z as shown in Eq. (4).

From the model, it can be seen that the resistance of the high-R layer should be controlled within the proper range. If the resistance is chosen to be too low, the resistance from the hetero junction will consume a large proportion of the applied voltage. However, if the resistance of the Hi-R layer is too large, only a small proportion of the current can reach the

center region if V_1 is higher than V_0 . These two situations both result in no phase retardation in the central region.

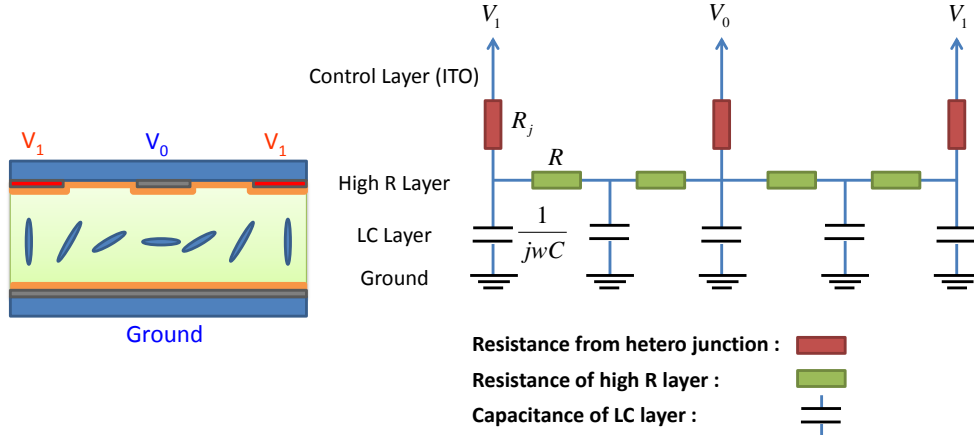


Fig. 4. The R-C circuit model of the high-resistance LC lens.

$$R = \frac{\rho_r}{A_r} l_r = \frac{\rho_r}{t_r w_r} l_r = R_s \frac{l_r}{w_r} \quad (1)$$

where ρ_r is the resistivity of the Hi-R layer. A_r and l_r are the cross section and length of the resistance. R_s is the sheet resistance.

According to the equation, to have an optimized distribution of gradient voltage, the range of resistivity of the Hi-R layer is from 1 to 10 $\Omega \cdot m$.

$$P_z = |\overline{P}_{\parallel}| \sin \theta + |\overline{P}_{\perp}| \cos \theta = \varepsilon_0 (\chi_{\parallel} \sin^2 \theta + \chi_{\perp} \cos^2 \theta) E \quad (2)$$

$$\chi_z = \frac{P_z}{\varepsilon_0 E} = \chi_{\parallel} \sin^2 \theta + \chi_{\perp} \cos^2 \theta \quad (3)$$

$$C = \frac{\varepsilon A}{d} = \frac{1 + \chi_z}{d} A \quad (4)$$

where d and A are the thickness and area of the meshed element, respectively.

2.3 Rotatable lenticular LC lens

Because of the increasing popularity of portable devices, the rotatable functionality of a display in 3D mode has become a requirement that must be considered. To achieve rotatable functionality in a lenticular LC lens, the two sets of stripe electrodes should be arranged in different directions. The structure is shown in Fig. 5 (a). However, when we apply a voltage to a top or bottom electrode in this structure, there is no full flat electrode on the other side. According to the structures and electrode fields of the LC cell, the LC cell will not behave as a lenticular lens. To form the shape of a lenticular lens, the variation of the electrode field should be changed only in one direction. The high-resistance layer can be used to overcome this issue.

According to the switchable functionality of the electrodes, we propose a rotatable lenticular LC lens with a high-resistance coating on both inner electrodes. To form a lenticular lens in two directions, the top electrodes and the bottom electrodes should be nearly perpendicular to each other. To achieve switchable functionality in two directions, the top and bottom electrodes are coated with high-resistance material, as shown in Fig. 5 (b). When all

bottom electrodes are connected to V_{com} and the top electrodes are driven by alternating voltages, V_D and V_{com} , an LC lenticular lens shape will form in the horizontal direction, as shown in Fig. 5 (c). Because of the application of the same driving voltage on each electrode, the bottom electrodes behave as a full electrode with the ground voltage. However, the voltage distribution on the top side becomes a gradient and continuous distribution because of the function of the high-resistance layer.

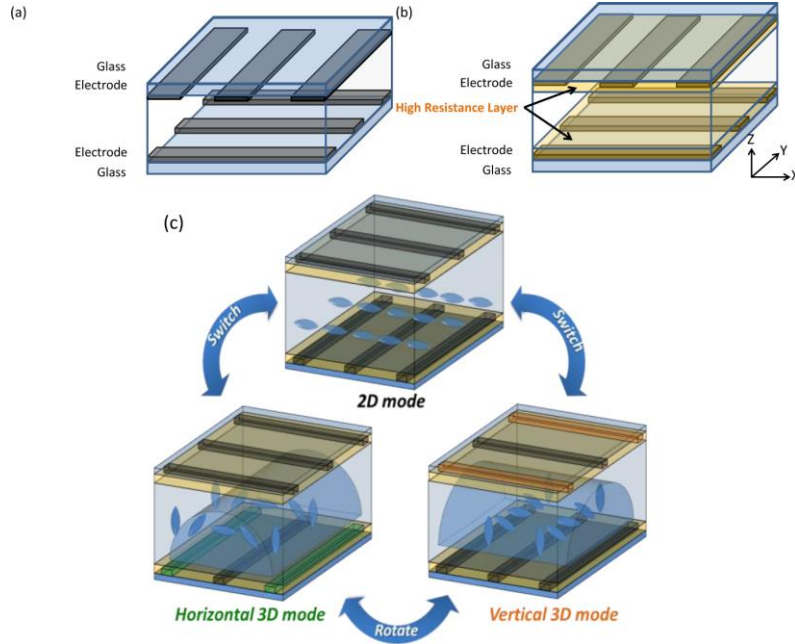


Fig. 5. Sketch of the rotatable high-resistance liquid-crystal lens (Hi-R LC lens): (a) without high-resistance layer, (b) with high-resistance layer, (c) the structure in the X-Z(horizontal) plane, and Y-Z(vertical) plane.

Furthermore, in the vertical direction, the LC lens can be operated in the same manner, as shown in Fig. 5 (c). The bottom electrodes are driven by V_D and V_{com} alternately, and all electrodes on the top are driven by V_{com} .

3. Experimental results

3.1 Specifications

We designed the Hi-R LC lens to generate 2 views of an autostereoscopic image in the vertical direction on an LCD panel and 4 views of an autostereoscopic image in the horizontal direction on the same panel. The specifications and parameters are shown in Table 2.

Table 2. Specification of Hi-R LC Lens and Panel

Item	Value
LC material	MLC-2140
Δn	0.253
Cell gap	50 μm
Focal length	1.17 mm
Electrode width	15 μm
Resistance material	IGZO
Thickness of high-R layer	10 nm
Resistivity	4.6 $\Omega \cdot m$
Pixel size	153 μm
Driving Voltage (2 views)	2 volts
Driving Voltage (4 views)	1.5 volts
Power Consumption	0.02 mW

3.2 Fringe pattern

To prove the effect of the high-resistance layer, a fringe pattern is an obvious method of demonstrating the result of the LC phase. In Fig. 6, the operated LC cell is observed under a crossed polarizer; the alternate white and black patterns represent the phase variations. Here, V_D and V_{com} are 2 and 0 volts, respectively. And the waveforms were square wave with constant 1 KHz frequency. The phase variation in the LC lens without the Hi-R layers is discontinuous and bent under the horizontal electrodes, as shown in Fig. 6 (b). Because V_{com} is applied only on the electrodes of the bottom substrate, the electric field cannot reach the centers of the slits between the electrodes. Thus, the electric fields of the vertical electrodes bend strongly toward the horizontal electrodes. Therefore, without the Hi-R layers, the electric-field distribution cannot form a lenticular LC lens profile.

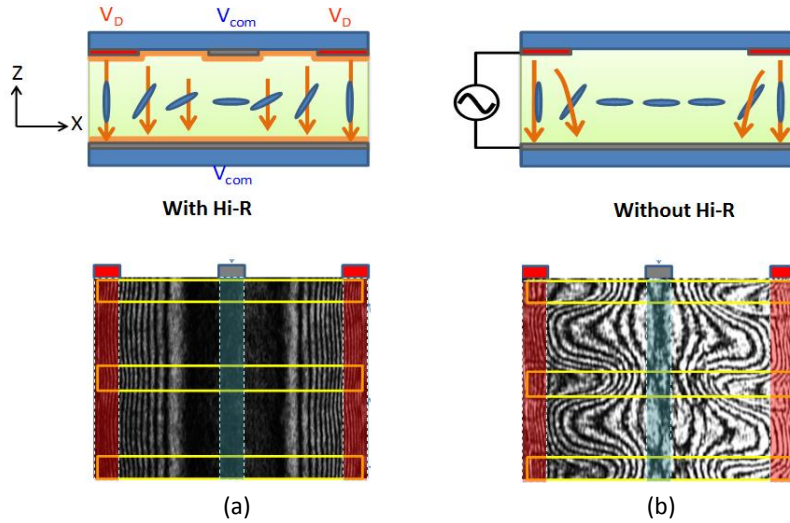


Fig. 6. The experimental results of a fringe pattern in a cross-electrode LC lens (a) with high-resistance layers and (b) without high-resistance layers.

In contrast, the fringe pattern in the Hi-R LC lens exhibits a continuous and smooth phase variation, so it can produce a good lens shape, as shown in Fig. 6 (a). The result demonstrates that the n_{eff} does not change gradually near the positions of the electrodes. Although there is a high-resistance layer, the electrode and high-resistance layer are connected in parallel. This means that the effective resistance must be smaller than the total resistance of the electrode, and the Hi-R layer, so the electrode will interfere with the driven gradient.

Therefore, a narrower electrode width will generate better performance. The electrical fields propagate smoothly from the vertical electrode to the planar electrode, which is a horizontal electrode coated with a Hi-R layer. Therefore, the phase distribution of the lenticular lens in the Hi-R LC cell is better than that in the LC cell without Hi-R layers.

3.3 Rotatable function

To demonstrate the 2D/3D switchable and rotatable functionalities on the same LC lens, the focusing ability becomes a criterion by which to judge the direction of the lenticular lens. The focusing ability of the Hi-R LC lens can be observed by using a parallel light, and the CCD locate at the focal plane of LC lenticular lens. When the parallel light passes through an LC cell voltage applied to the cell, there is no significant pattern on the CCD, as shown in Fig. 7 (a). If the driving voltage is applied along the vertical direction of the cell, the LC lenticular lens array forms in the horizontal direction. Therefore, the focused lines appear on the CCD as shown in Fig. 7 (b). The result is similar when the driving voltage is applied to the horizontal electrodes; the LC lenticular lens array forms in the vertical direction, as shown in

Fig. 7 (c). The full video is available at the following web address: <http://youtu.be/5LA9o0XPABw>.

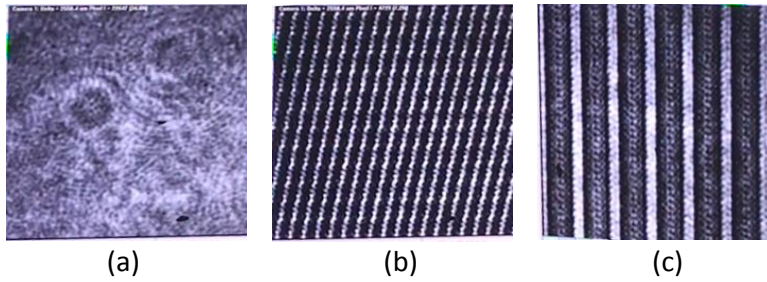


Fig. 7. Test of the focusing ability the Hi-R LC Lens: (a) without any driving voltage, (b) operating the Hi-R LC lens in the horizontal direction, and (c) operating the Hi-R LC lens in the vertical direction (Media 1).

3.4 Angular crosstalk distribution

The angular distribution of the 2D/3D switchable autostereoscopic display achieved by operating the Hi-R LC lens array in the horizontal direction is shown in Fig. 8. The Hi-R LC lens simulation results indicate that defects near the electrodes cause leakage. The width ratio of all electrodes and lenses corresponds to a pitch of approximately 0.3. This defect will cause a high crosstalk in 3D mode. When the cell is operated at 1.5 volts, the multi-view crosstalk in the horizontal direction is 34.3%, as shown in Fig. 8 (b). In the vertical direction, the width ratio of all electrodes and lens corresponds to a pitch of approximately 0.06, as shown in Fig. 8 (a). When the cell is operated at 2 volts, the crosstalk in the vertical direction is 9.8%.

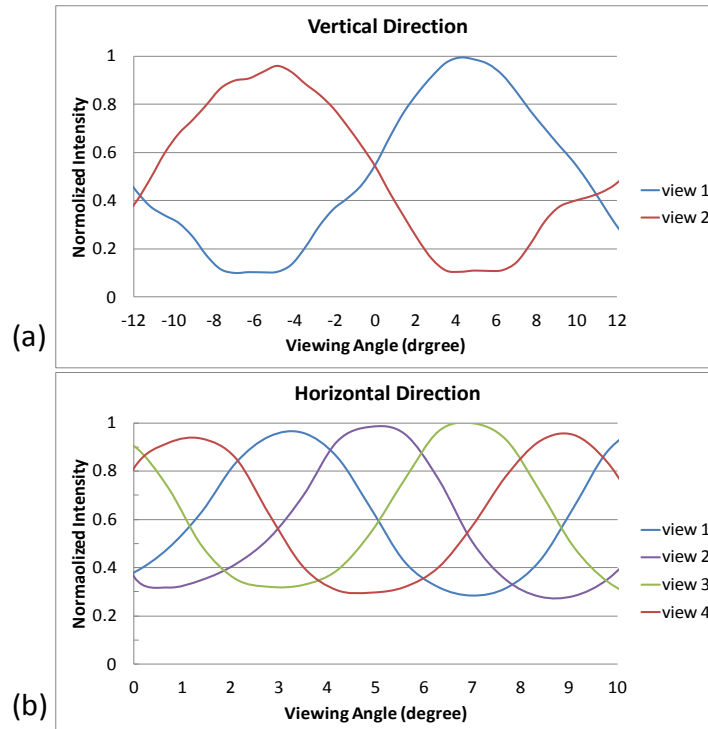


Fig. 8. The angular distribution of the Hi-R LC Lens in (a) the vertical direction and (b) the horizontal direction.

Table 3. Specification of Hi-R LC Lens on Simulation

Item	Value
LC material	MDA-00-3461
Δn	0.257
Cell gap	50 μm
Lens Pitch	100 μm

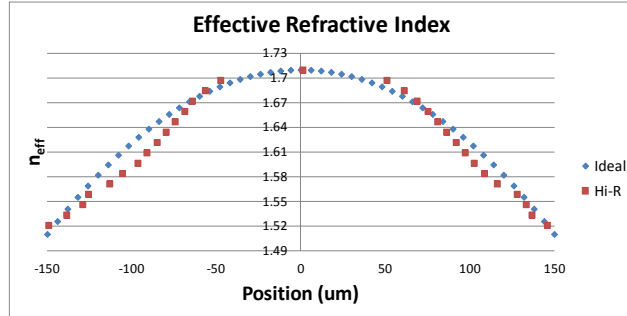


Fig. 9. The comparison of the effective refractive index between ideal lens and Hi-R LC Lens.

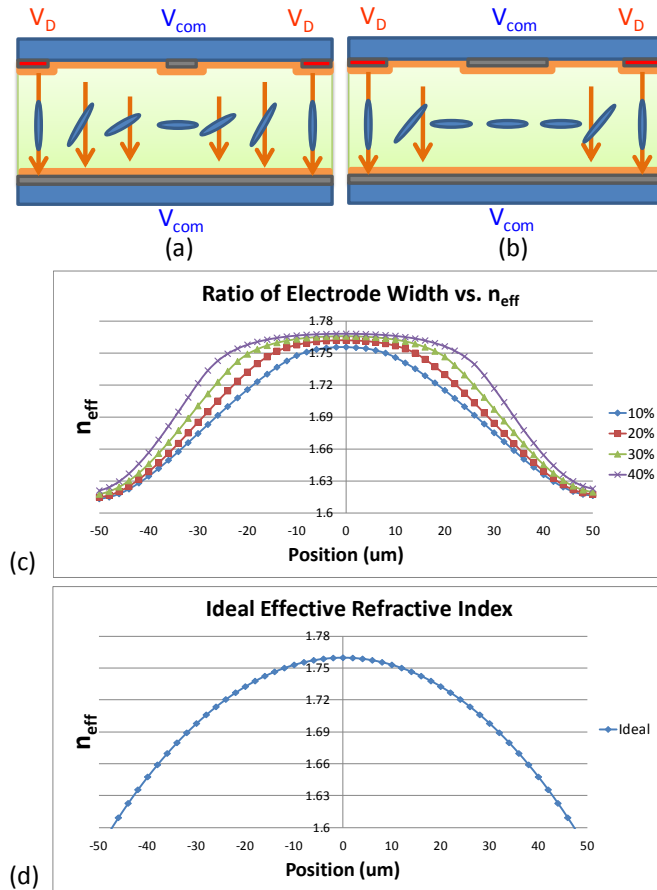


Fig. 10. The influence of the ratio of electrode width on the effective refractive index (n_{eff}): (a) structure of low ratio of electrode width, (b) structure of high ratio of electrode width, (c) various ratios of electrode width and (d) the ideal case.

To find out what is the reason will cause the crosstalk on Hi-R lens, the effective refractive index (n_{eff}) is measured and show on Fig. 9. Compare with the profile of ideal lens, the distribution of n_{eff} is too flat at the center and the edge of LC-lens. Therefore, the light will not refract to the designed angle. We believe this phenomenon comes from the electrode width of the Hi-R LC lens. Because of manufacturing limitations, the electrode width of the Hi-R LC lens of our sample is around 15 μm . According to these parameters, the effective refractive index was simulated using 2DiMOS. The ratio of electrode width to lens size varies from 10% to 40%, and the sketch is shown on Fig. 10 (a) and (b). The parameters of LC lens on simulation are shown in Table 3. The result indicates that the n_{eff} does not change gradually near the position of the electrode, as shown in Fig. 10 (c). Although there is a high-resistance layer, the electrode and the high-resistance layer are connected in parallel. This means that the effective resistance must be smaller than the total resistance of the electrode and the Hi-R layer, and the electrode will interfere with the driven gradient. Therefore, a narrower electrode width will generate better performance. Figure 10 (d) shows the n_{eff} distribution of an ideal Hi-R LC lens with a very small electrode width. Therefore, lower crosstalk could be achieved if narrower electrodes were used. The 5 μm electrode width can be easily achieved by conventional TFT-LCD company, thus shall be able to yield much lower crosstalk for the dual-directional Hi-R LC-lens.

3.5 Response time

To fit the power of the lens, the cell gap of LC Lens is 50 μm in our experiment. According to rising time, τ_{rise} of LC devices, larger cell gap results in slow focusing time which is proportional to d^2 from relaxing state to focusing state, as Eq. (5) shows.

$$\tau_{\text{rise}} = \frac{\gamma_1 d^2 / K \pi^2}{(V / V_{th})^2 - 1} \quad (5)$$

where τ_{rise} is the function of cell gap d , rotational viscosity γ_1 , elastic constant K , threshold voltage V_{th} , and applied voltage V . To overcome slow response of LC cells, over-drive is employed for accelerating the response times in LCD industry. By optimized the over driving voltages and switching to target operation, the LC response time can be much reduced. In our experiment, the optimized over-drive value is about 4 volts, and the rising time is close to 0.6 second. Figure 11 shows the sequential photograph of LC lens form non-focusing to focusing on different period.

To fit the power of the lens, the cell gap of LC Lens is 50 μm in our experiment. According to rising time, τ_{rise} of LC devices, larger cell gap results in slow focusing time which is proportional to d^2 from relaxing state to focusing state, as Eq. (5) shows.

$$\tau_{\text{rise}} = \frac{\gamma_1 d^2 / K \pi^2}{(V / V_{th})^2 - 1} \quad (6)$$

where τ_{rise} is the function of cell gap d , rotational viscosity γ_1 , elastic constant K , threshold voltage V_{th} , and applied voltage V . For current LCD, which has cell gap around 5 μm , the response time is about 6ms with over-driving technology [34]. According to the listed equation, LC-lens with 50 μm cell gap shall be around $6\text{ms} \times 10^2 = 600\text{ms}$. In our experiment, the optimized over-drive value is about 4 volts, and from the experiment results, our rising time is close to 600ms which is similar to the theoretical calculation. Figure 11 shows the sequential photograph of LC lens form non-focusing to focusing on different period.

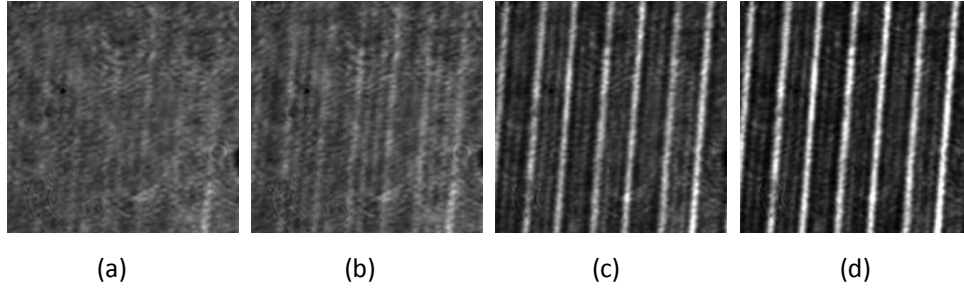


Fig. 11. The sequential photograph of focusing of LC lens driven by over-drive method: (a) 0 sec, (b) 0.2 sec, (c) 0.4 sec and (d) 0.6 sec.

4. Conclusion

A High-Resistance Liquid Crystal (Hi-R LC) lens that is capable of 2D/3D switching and 3D rotation is proposed. Using high-resistance layers, a continuous gradient electric-field distribution can be generated within the cell. Consequently, high-quality 3D images for horizontal and vertical viewing can be obtained. In our prototype, the crosstalk of the two-view system is below 10%, but in the rotated direction, the crosstalk of the multi-view system is approximately 34.3% because of the slanted 4-view design, but could be much improved by narrowing the electrode width. The Hi-R LC lens requires only a low operating voltage and a simple driving system. Finally, the Hi-R LC lens was successfully implemented on an LCD for 2D/3D switching and 3D rotation functionality, thereby demonstrating its high potential for application in future mobile autostereoscopic displays.

Acknowledgments

This work was partially supported by the National Science Council, Taiwan, for Academic Projects No. NSC101-2221-E-009-120-MY3.